Electrochemical and spectroelectrochemical studies of tert-butyl-substituted aluminum phthalocyanine

Electrochemical and spectroelectrochemical studies of *tert*-butyl-substituted aluminum phthalocyanine

Ekaterina O. Moiseeva[a], Stanislav Trashin[c], Yuliya S. Korostei[b], Shahid Khan[c], Kosov D. Anton[a], Karolien De Wael[c], Tatiana V. Dubinina[a], Larisa G. Tomilova [a, b †]

a. *Department of chemistry, Lomonosov Moscow State University, 119991 Moscow, Russian Federation.*

b. Instituite of physiologically Active Compounds, Russian Academy of Science, 142432 Chernogolovka, Moscow Region, Russian Federation.

c. AXES research group, Groenenborgerlaan 171, University of Antwerp, 2020 Antwerp, Belgium.

@Corresponding author E-mail: ekaterina.moiseeva@chemistry.msu.ru

Abstract

Tetra-*tert*-butylphthalocyanine aluminum (III) chloride was studied by voltammetric and potential-resolved spectroelectrochemical methods in a non-coordinating solvent *o*-dichlorobenzene. Five redox transitions were found including two oxidation waves at 0.18 and 0.90 V and three reduction waves at −1.28, −1.65, and −2.63 V vs. Fc^+/Fc. Electrochemical reversibility of the first oxidation and reduction processes was assessed by using the diagnostic criteria of cyclic voltammetry. First comprehensive spectroelectrochemical characterization of oxidation of the aluminum phthalocyanine is reported. Moreover, potential-resolved spectroelectrochemical titration revealed strong influence of aggregation on the UV-vis spectra and the half-wave potentials of the first oxidation transition and disclosed the presence of the partially oxidized complex in the initial solution, which noticeably affected the spectrum of the neutral form.

Key words: aluminum phthalocyanine, electrochemical reversibility, aggregation, electrochemistry, spectroelectrochemistry.

Introduction

A phthalocyanine (Pc) macrocycle has a planar 18 π-electrons aromatic system with peculiar optical and redox properties that can be largely influenced by peripheral substituents and the central metal ion [1]. Trivalent metals (e.g., Al, Ga, In) additionally coordinate an axial ligand such as chloride, fluoride, hydroxide, phenolate and others [2-4]. Aluminum (Al^{3+}) with a high charge density due to its small size is of special interest because of its strong impact on charge distribution in the Pc macrocycle and the axial ligand. Aluminum phthalocyanine complexes were shown to be promising in the field of catalytic synthesis of cyclic carbonates from carbon dioxide [5, 6] and other carbonylation reactions [7], photodynamic therapy of cancer [8], photocatalysis [9], bulk-heterojunction solar cells [10, 11] and as molecular switches [12, 13]. The ability to coordinate an axial ligand plays a crucial role in preparation of ordered Pc thin films [14] with improved photoelectrochemical properties [15] and in synthesis of hybrid nanostructures due to the axial ligand substitution reaction [16].

Electrochemical behavior of unsubstituted aluminum Pc was the subject of several studies. Cissell et al. [17] studied the electrochemical reduction of PcAlCl in THF in comparison to chemically reduced and isolated $[PcAl]^0$ without any axial ligand. The data suggests that Cl^- as the axial ligand strongly affects the formal potential for the transition $[PcAlCl]/[PcAlCl]^-$ shifting it by 0.30 V towards a lower value compared to the transition $[PcAl]^+/[PcAl]^0$. However, the formal potential for the second reduction (*i.e.*, $[PcAlCl]^-/[PcAlCl]^{2-}$) exactly matches the formal potential for $[PcAl]^0/[PcAl]^-$ indicating that Cl^- anion dissociates from the one-electron reduced form $[PcAlCl]^-$. The same conclusion was reported by Ou et al. in their detailed study of the electrochemical reduction of PcAlCl in different conditions and solvents [18]. They observed a strong effect of coordinating solvents on the second reduction potential of PcAlCl. It was shown that pyridine shifts the second reduction potential by 0.15 V to more negative potentials compared to THF likely owing to stabilization of two-electron reduced $[PcAl]^-$ by pyridine via its coordination to the metal center. The authors also demonstrated that the first reduction potential (but not the second or the third reduction potential) of PcAlCl is sensitive to the presence of Cl^- and other anions in the solution.

In an older study [19], the authors compared the first oxidation and first reduction potentials of PcAlCl with those of PcZn and PcMg complexes in DMF and DMA. In both works, the metal center in PcAlCl shows a strong electron-withdrawing effect shifting the oxidation and reduction potentials by 0.3—0.4 V towards more positive values. Noteworthy, the electrochemical HOMO-LUMO energy gap ($\Delta E = E_{Red} - E_{Ox}$) remains the same in both solvents and does not depend on the metal center. Lever and Minor [20] reported a first reduction and oxidation potentials of PcAlCl in DMF.

The electrochemical behavior of aluminum Pcs in the oxidation region and in non-coordinating solvents was poorly represented in the literature. However, voltammetric behavior of PcAlCl in a non-coordinating solvent CH_2Cl_2 [21] showed irreversibility of the first oxidation and first two reduction transitions with the first oxidation peak at a potential shifted by *ca.* 0.45 V from the value in THF and DMF, which is rather high. Poor reversibility may result from poor solubility and high aggregation of unsubstituted PcAlCl in non-coordinating solvents and can be addressed by introducing bulky peripheral groups such as *tert*-butyl or *iso*-propyl groups. Lapok's et al. reported on electrochemical behavior of PcAlCl substituted with bulky fluorinated *iso*-propyl groups in comparison with analogous In and Ga complexes [22]. Due to the electron-withdrawing effect by florin, no oxidation of the complexes was observed within the available potential window in THF and all reduction potentials were noticeably shifted (by *ca.* 0.8 V) towards more positive values in respect to the formal potentials of PcAlCl [23]. A short communication on the spectroelectrochemical and electrochemical oxidation of ^{tBu}PcAlCl in acetonitrile [24] lacks important details including clear assignment of the potential scale which is needed for comparison with other works. Nevertheless, reduction and oxidation potentials for alkyl substituted Pc complexes of indium and gallium were reported [25, 26].

In this work, we conducted voltammetric and spectroelectrochemical studies of *tert*-butyl-substituted Al phthalocyanine (^{tBu}PcAlCl) in a non-coordinating solvent *o*-DCB. The bulky *tert*-butyl groups were introduced at the peripheral positions to increase solubility and lower aggregation of the complex in organic solvents [27, 28]. This is the first detailed electrochemical study of an aluminum phthalocyanine in a non-coordinating and the first detailed spectroelectrochemical study that particularly revealed influence of aggregation in the neutral and oxidized forms on electrochemical and UV-Vis spectral properties.

Materials and Methods

All reagents and solvents were obtained or distilled according to standard procedures. Aluminum chloride (Sigma-Aldrich, reagent grade) were used as received. Matrix assisted laser desorption/ionization time-of-flight (MALDI-TOF) mass-spectra were taken on a Bruker Autoflex II mass spectrometer with α-cyano-4-hydroxycinnamic acid (CHCA) as the matrix. The crude 2(3),9(10),16(17),23(24)-*tert*-butylphthalocyanine aluminum (III) chloride was prepared by heating a mixture of anhydrous aluminum chloride and 4-*tert*-butylphthalonitrile to 270 ^{o}C 3 hours in accordance with the known procedure [29]. Purification was achieved by sublimation in vacuum. The MALDI-TOF and FT-IR spectra performed in Fig. S1 and Fig. S2 respectively. UV-Vis THF/nm (lg ε): 681 (5.36), 613 (4.60), 360 (4.86); MS (MALDI-TOF) m/z: 798.070 ([M^-], 100%), calculated for $C_{48}H_{48}N_8AlCl$: 798.35 (100.0%); FT-IR (KBr): ν (cm^{-1}) = 2950-2810 (CH st), 1600 (γ pyrrole).

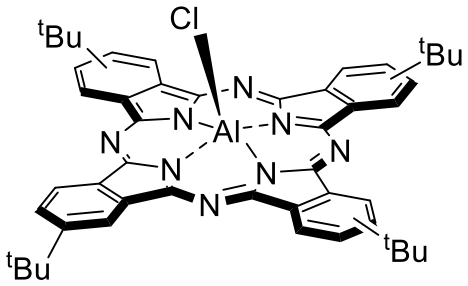

Figure 1. Structure of tetra-*tert*-butylphthalocyanine aluminum (III), ^{tBu}PcAlCl.

Electrochemical measurements were carried out with Autolab PGSTAT302N controlled by Nova 1.11 (Metrohm Autolab B.V., The Netherlands). Cyclic voltammetry (CV) and square wave voltammetry (SWV) were performed in a conventional three-electrode cell with Pt-disk (2.0 mm in diameter) working and Pt-rod counter electrodes. *o*-Dichlorobenzene (*o*-DCB, 99%, J&K) containing 0.1 M $TBAClO_4$ (Sigma-Aldrich) was used as supporting electrolyte. A double junction Ag/AgCl reference electrode (Metrohm 6.0726.100) was filled with 2 M LiCl in EtOH as the inner solution and the supporting electrolyte as the bridge solution. To correct a liquid junction potential, all potentials were referred to the ferrocenium$^+$/ferrocene (Fc^+/Fc) couple (0.584 ± 0.005 V vs. Ag/AgCl used). The working solution was purged with argon before measurements for at least 20 min.

UV-Vis absorption spectra were recorded on a Jasco V-770 spectrophotometer using quartz cells (optical path of 1.00 cm). Spectroelectrochemical studies were conducted with Avantes AvaSpec 2048 spectrometer coupled with Autolab 101 potentiostat/galvanostat (Metrohm-Autolab) using a thin-layer quartz spectroelectrochemical cell (optical path of 1.0 mm) containing a Pt-mesh working, Pt-wire counter and Ag/Ag^+ reference electrodes. *o*-Dichlorobenzene (*o*-DCB, 99%, J&K) was used as a solvent with 0.1 M $TBAClO_4$ (Sigma-Aldrich) as the supporting electrolyte. The potential of the Ag/Ag^+ reference electrode was compared with the Ag/AgCl reference electrode used in the voltammetric studies. All potentials were recalculated to be given relative to the Ag/AgCl reference electrode for consistency. The potential was varied stepwise with a potential step of 0.05 V and the electrolysis time for each step of 5 min resulting in an apparent scan rate of 0.17 mV/s.

Results and discussion

Spectroscopic characterization

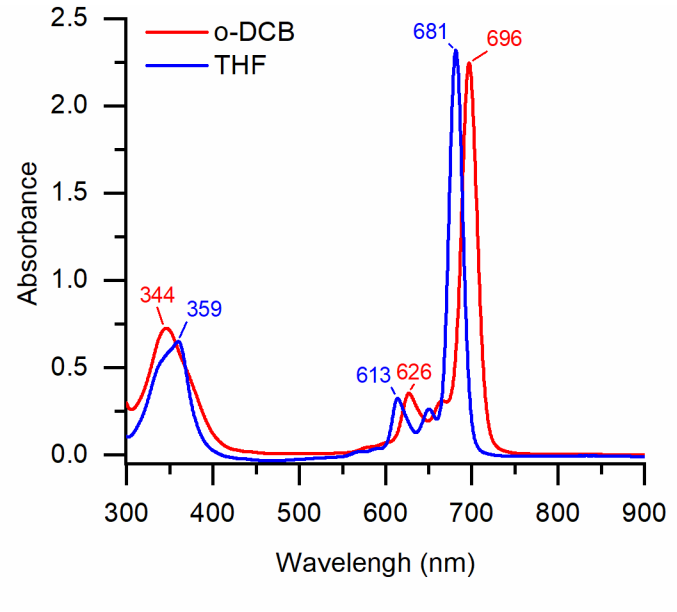

Figure 2. UV-Vis absorption spectra of ^{tBu}PcAlCl (c ~ 0.01 mM) in *o*-DCB (red) and THF (blue).

The absorption spectrum of non-aggregated metal phthalocyanines typically shows two major sets of bands, Q and B bands. The Q band is more intense and located in the visible region (600 – 700 nm), whereas the B band is located in the UV region (around 350 nm). Along with the satellite Q_{vib} at around 620 nm, the Q band is highly sensitive to peripheral substituents, the central metal, solvents and aggregation due association with the HOMO-LUMO transition [30]. The UV-Vis spectrum of ^{tBu}PcAlCl in THF (Fig. 2) represents a typical spectrum of a monomeric neutral Pc [1] with absorption bands at 359, 613, 650 and 681 nm. The intense Q band and well-resolved satellite indicated lack of aggregation in this solution. The Q band of ^{tBu}PcAlCl is expectedly shifted by 6 nm towards higher wavelengths compared to the unsubstituted analogue PcAlCl in the same solvent (absorbance maxima at 347, 609, 642 and 675 nm) [18], which corresponds well to the electron-donating effect of tBu-groups. In contrast to unsubstituted PcAlCl, ^{tBu}PcAlCl is well soluble in *o*-DCB, a non-coordinating solvent with a comparatively high refractive index. As previously reported in the literature, aromatic solvents especially with a high refractive indexes result in a red shift in the Q band [31], which was 15 nm compared to the solution in THF in our case (696 nm in *o*-DCB and 681 nm in THF).

Electrochemical characterization

CVs and SWVs of ^{tBu}PcAlCl in *o*-DCB and solution containing $TBAClO_4$ as supporting electrolyte are shown in Fig. 3. SWVs of ^{tBu}PcAlCl in *o*-DCB/ $TBAClO_4$/pyridine are shown in Fig. S3. Table 1 lists the formal potentials (E°') of

redox transitions of ^{tBu}PcAlCl/TBClO$_4$ in *o*-DCB and o-DCB/ TBClO$_4$/pyridine. The literature data for PcAlCl in different solvents and electrolytes are given for comparison. All transitions of ^{tBu}PcAlCl in *o*-DCB were expectedly shifted by 1.0 V towards more negative values in comparison with a fluorinated complex ^{F64}PcAlCl and by 0.1—0.2 V in comparison with unsubstituted PcAlCl (Table 1). In other words, the compound oxidizes easier and reduces harder compared to unsubstituted PcAlCl and the fluorinated complex in agreement with the electron-donating effect of *tert*-butyl groups.

Noteworthy, adding a small amount of pyridine to *o*-DCB (final 5 vol% pyridine) shifted the first oxidation peak by 0.10 V towards a more positive potential, while the formal potential for the first and second reduction transitions remained generally the same (Table 1). The influence of pyridine suggests either coordination of the central metal with pyridine or disaggregation of the complex in the presence of pyridine additive. Substitution of the axial Cl^- in coordinating solvents was previously observed for the one-electron reduced but not the initial neutral form of PcAlCl [23]. Moreover, Red_1 and Red_2 do not shift noticeably as could be expected in case of dissociation of the axial Cl^- [17]. Thus, the partial aggregation of the neutral form is most likely, whereas the Cl^- should not dissociate in our conditions. Moreover, it is known that addition of a drop of pyridine in phthalocyanine solutions in general improves resolution of UV-Vis and NMR spectra [32-34] apparently due to decrease of aggregation.

Table 1. Oxidation/reduction potentials ($E^{o\prime} \pm 0.01$ V vs. Fc^+/Fc) and the electrochemical HOMO-LUMO gaps (the difference between first oxidation and reduction potentials, ΔE).

Complex	Solvent/electrolyte	Red_3	Red_2	Red_1	Ox_1	Ox_2	ΔE	Ref
^{tBu}PcAlCl	o-DCB/TBAClO$_4$	−2.63	−1.65	−1.28	0.18	0.90	1.46	tw
^{tBu}PcAlCl	o-DCB/TBAClO$_4$/py		−1.68	−1.30	0.28		1.58	tw
^{F64}PcAlCl[a]	THF/TBABF$_4$	−1.03	−0.54	−0.28				[35]
PcAlCl	THF/TBAPF$_6$		−1.55	−1.15				[17]
PcAlCl	DMF/TEAClO$_4$			−1.15[b]	0.42[b]		1.57	[36]
PcAlCl	THF/TBAClO$_4$	−2.46	−1.58	−1.11				[23]
PcAlCl	DCM/TBAClO$_4$	−1.93[c]	−1.49[c,d]	−1.24[c,d]	0.87[c,d]		-	[21]

tw – this work. [a]$_{F64}$PcAlCl = 1,4,8,11,15,18,22,25-octafluoro-2,3,9,10,16,17,23,24-octakis(perfluoroisopropyl)phthalocyanine. [b]The potentials were recalculated from values given vs. SCE using $E^o(Fc^+/Fc) = 0.50$ V vs. SCE in DMF [37] . [c]The potentials were recalculated from values given vs Me10Fc+/ Me10Fc+ to be vs Fc+/Fc. $E^o(Fc+/Fc) = 0.532$ V vs. $Me_{10}Fc^+$/ $Me_{10}Fc$ in DCM [38]. [d]Irreversible peaks.

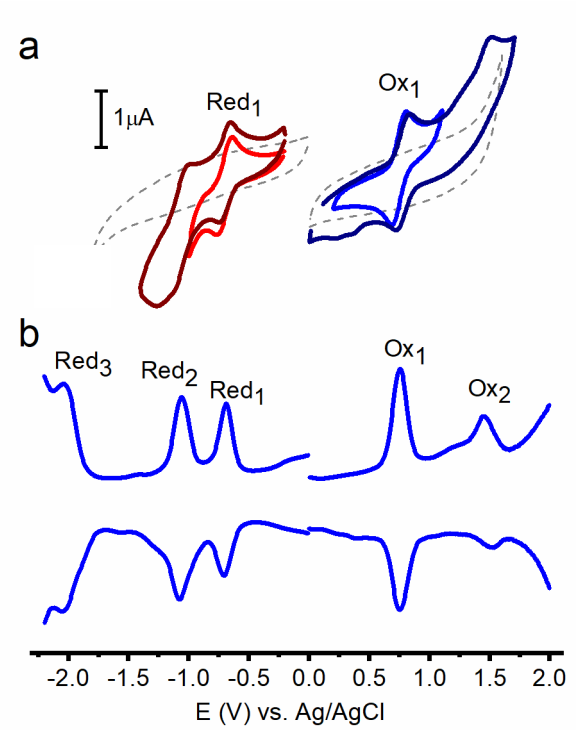

Figure 3. (a) Cyclic and (b) square wave voltammograms of ^{tBu}PcAlCl (0.6—1.0 mmol/l) at a Pt-disk electrode in *o*-DCB/TBAClO$_4$; CVs scan rate: 100 mV/s. SWV amplitude 50 mV; step potential, 5 mV.

More detailed analysis of the cyclic voltammetry data showed that Ox$_1$ (ΔE_p = 110 mV, $i_{p,a}/i_{p,k}$ = 0.96) and Red$_1$ (ΔE_p = 110 mV, $i_{p,a}/i_{p,k}$ = 0.88) transitions are quasi-reversible, whereas the second oxidation Ox$_2$ is rather irreversible. Moreover, the measurements with the upper vertex potential above the second oxidation resulted in partial passivation of the back reduction peak Ox$_1$. This agrees with the irreversible nature of Ox$_2$ that may form species adsorbed on the electrode leading to the electrode fouling. Nevertheless, representative voltammograms for Ox$_1$ could be practically obtained by limiting the upper vertex potential or introducing a gentle stirring of the solution. The potential gap between the first oxidation and reduction ΔE = E(Ox$_1$) – E(Red$_1$) = 1.46 V was similar to ΔE reported for ^{tBu}PcZn [39] and slightly lower than ΔE obtained for PcAlCl in THF (Table 1). Electrochemical study of PcAlCl in DCM showed only irreversible processes with irreversible peaks at potentials noticeably shifted from the expected values, which does not allow to estimate accurately the formal potentials in these conditions [21].

In order to investigate the electrochemical reversibility of the first oxidation and reduction transitions and to exclude the presence of side reactions at the electrode, we applied the diagnostic criteria of voltammetry for characterization a quasi-reversible electron transfer reaction. Voltammograms were recorded within the limited potential windows at different scan rates for detailed characterization of the first oxidation or first reduction transitions (Fig. 4a, d). Fig. 4b and e represents the dependence of the peak positions as a function of the

logarithm of the scan rate. The peak-to-peak separation increases with the scan rates above 0.1 V/s eventually resulting in a linear dependence of the peak potential on the scan rate. This indicates the quasi-reversible behavior of Ox_1 and Red_1 transitions with good electrochemical reversibility at a scan rate of 0.1 V/s and lower. The peak current for Ox_1 and Red_1 is near linear with the square root of the scan rate (Fig. 4c and f) suggesting involvement of freely diffusing redox species in the observed transitions in agreement with the Cottrell equation.

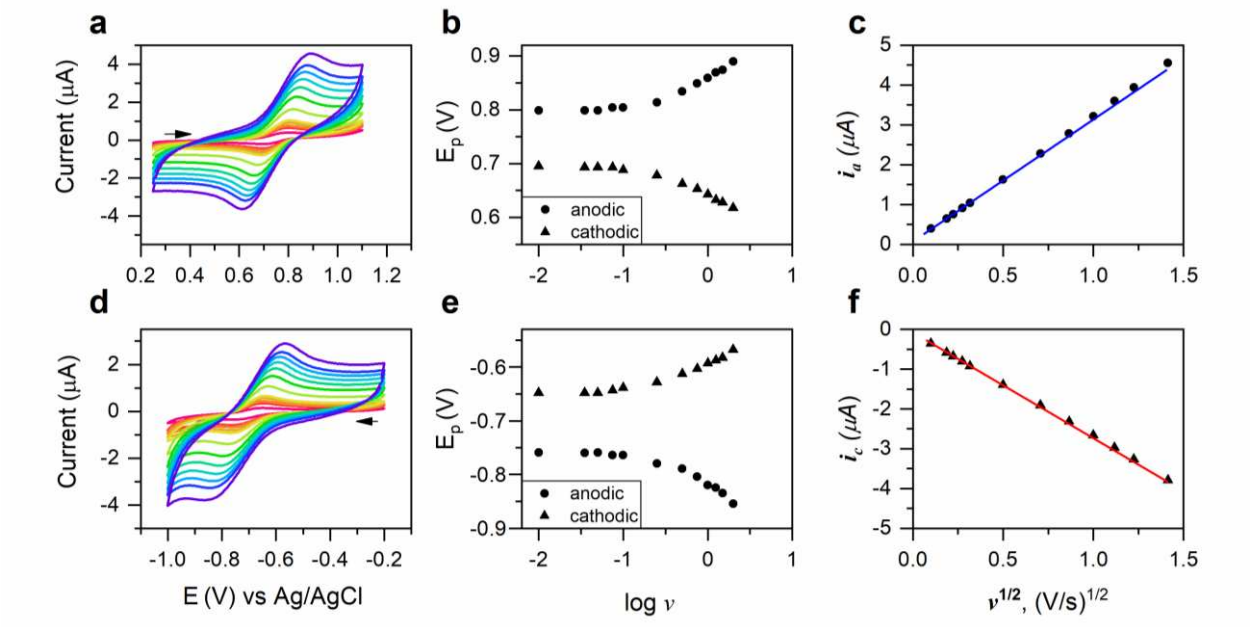

Figure 4. (a,d) Cyclic voltammograms of ^{tBu}PcAlCl in o-DCB/0.1 M $TBAClO_4$ at 0.01-2 V/s. (c,d) Trumpet plots of the peak potential, E_p, versus the logarithm of the scan rate, v. (c) Anodic peak current, i_a, and (f) cathodic peak current, i_c, plotted versus the square root of the scan rate v.

Spectroelectrochemical characterization

A more detailed study of the first oxidation transition Ox_1 was conducted using the stepwise potential-controlled spectroelectrochemical titration. This is the first detailed spectroelectrochemical investigation of oxidation of an Al phthalocyanine, whereas detailed spectroelectrochemical study for reduction of PcAlCl in THF was reported previously in the literature [23].

Fig. 5a represents spectral changes during electrochemical oxidation of ^{tBu}PcAlCl starting from an open circuit potential (OCP) value till 1.0 V with a step of 0.05 V. During the electrolysis, a decrease in absorbance of the Q and B bands and an increase of bands at 460, 548 and 860 nm occurred indicating formation of a π-cation radical $[ClAlPc^{-1}]^{\cdot+}$[36, 40, 41]. These bands positions and their relative intensity agree well with the spectra for the π-cation radical form of ^{tBu}PcZn with bands at 440, 500, 825 nm with much lower absorption compared to the Q and

B bands of the neutral form [42]. A clear set of isosbestic points at 328, 399 and 602 nm suggests a simple transformation between two forms. The halve-wave potential as obtained from the potential resolved titration curves (Fig. 5a inset) was 0.78 ± 0.01 V vs Ag/AgCl (0.20 V vs Fc^+/Fc) and corresponded well to the formal potential of 0.76 V obtained from CV (0.18 V vs. Fc^+/Fc, Table 1). Noteworthy, in a short communication in 1989 [24], the authors assigned three bands at 408, 535 and 850 nm to one-electron oxidized ^{tBu}PcAlCl in acetonitrile. However, the band at 408 nm was previously not observed in one-electron oxidized ^{tBu}PcZn in methylene chloride [42] and was not observed in this work, whereas two other bands matched well taking into account the solvent effect.

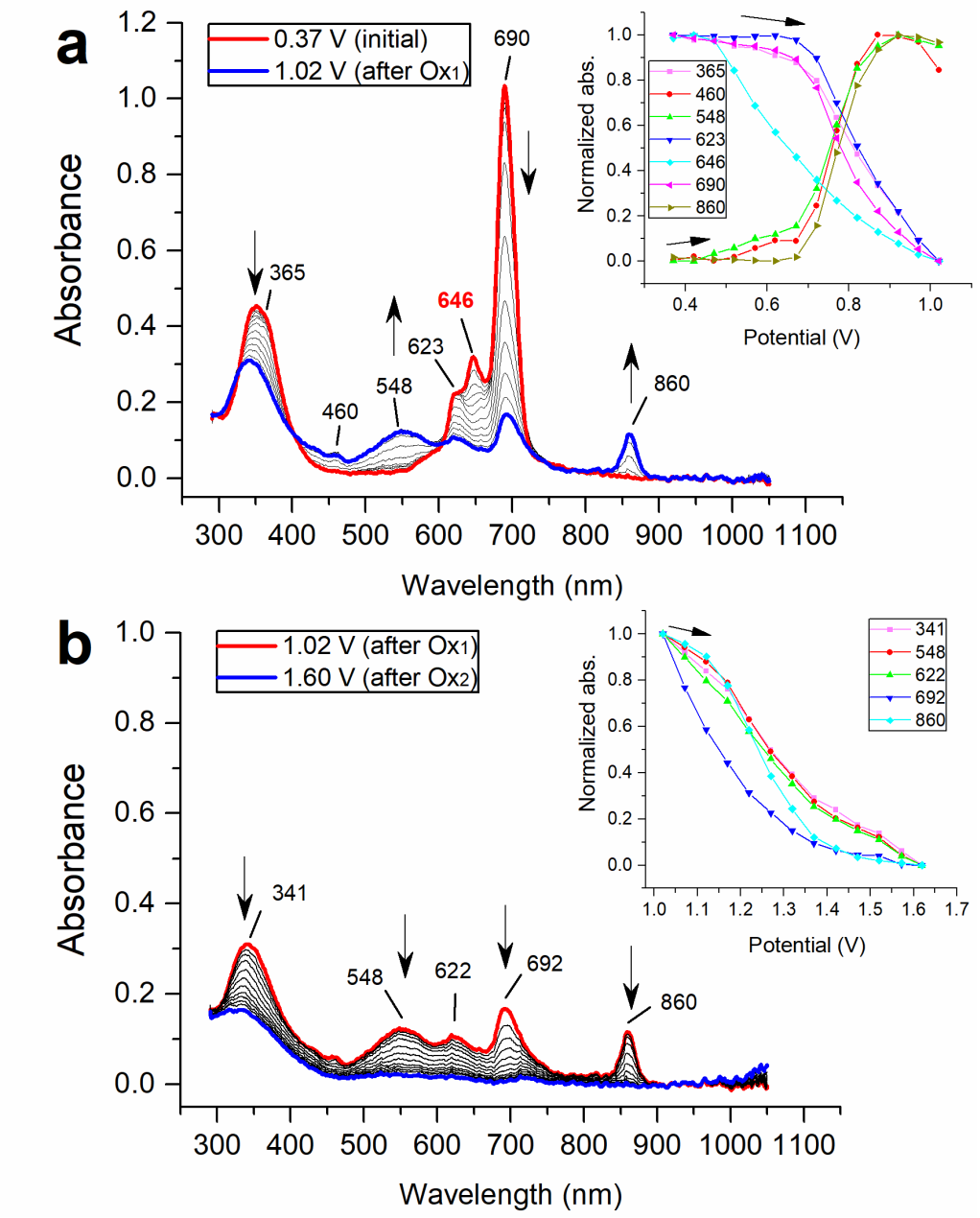

Figure 5. In-situ UV-Vis spectral changes of ^{tBu}PcAlCl (c ~ 0.15 mmol) in *o*-DCB containing 0.1 M $TBAClO_4$ in the region of the first oxidation transition Ox_1 (a) and the second oxidation transition Ox_2 (b).

As shown in Fig. 5b under conditions of the second oxidation (E_{app} varied from 1.00 to 1.60 V vs. Ag/AgCl) all bands dropped in intensity in agreement with irreversible decomposition of the macrocycle. The initial neutral form could not be recovered by backward electrochemical reduction from this two-electrons oxidized form. The half-wave potential was around 1.15 V vs. Ag/AgCl (0.57 V vs. Fc^+/Fc) as calculated for the Q-band at 692 nm and 1.26 V vs. Ag/AgCl (0.68 V vs. Fc^+/Fc) in average for the rest four radical-specific bands observed in the spectrum. These halve-wave potentials are lower than the first oxidation potential estimated from CV data by 0.30 V, which generally corresponds to an expected shift in a peak position in a voltammetric experiment for an electron transfer reaction complicated by a followed irreversible chemical process (e.g., irreversible decomposition of the phthalocyanine π-system) [43]. Thus, the observed oxidation process does not have an equilibrium state making the half-wave potential to be defined by the time-scale of the experiment (the effective scan rate is 0.16 mV/s for the spectroelectrochemical experiment). Peak positions obtained in comparatively fast voltammetric measurements (SWV and CV with a scan rate of 100 mV/s) as given in Table 1 should better estimate the formal potential for the second oxidation process in this case.

In general, the spectroelectrochemical data corresponded well to the typical ring-based UV-vis changes in the redox behavior of metallophthalocyanines having redox inactive metal center [44-46]. However, the peak at 646 nm behaved differently from other bands (Fig. 5a, inset). In particular, the changes were not as steep as for the main Q-band at 690 nm and started to drop already at the potential of 0.5 V vs. Ag/AgCl and dropped by 50% at 0.65 V, *i.e.* 0.11 V lower than the formal potential for Ox_1, 0.76 V vs. Ag/AgCl (0.18 V vs. Fc^+/Fc). This UV-vis band is usually associated with aggregates, which should be oxidized easier in comparison to the monomer [47]. Moreover, strong aggregation in the oxidized form may complicate spectroelectrochemical recovery of the complex. Indeed the main Q-band of the complex could not be fully recovered when the potential was gradually switched from 1.0 V to 0.3 V. Although the bands at 544 and 860 nm (characteristic to the cation-radical) disappeared and the Q-band satellite at 630 nm recovered, the main Q-band stayed low as expected in a strongly aggregated complex (Figure S4a, Supporting information). An additional study with octa-n-butyl-substituted analogue showed 70% recovery of the initial Q-band intensity in the same conditions owing to better solubility and stronger steric effects lowering the aggregation (Figure S4a, Supporting information). This additionally confirms that the chromophore is not destroyed after the first oxidation Ox_1.

Surprisingly, ^{tBu}PcAlCl showed noticeable spectral changes when the electrode potential shifted from the OCP value (0.32 V) by 0.5 V towards lower values (Fig. 6a). Although the potential reached −0.18 V vs. Ag/AgCl, it stayed much above than the first reduction potential (−0.70 V vs. Ag/AgCl). Thus, one-electron reduction of the neutral

macrocycles could not happen in these conditions. Nevertheless, the Q band shifted from 690 to 695 nm and slightly increased in intensity. The satellite at 646 nm (attributed to the H-aggregates) shifted to 640 nm and increased in intensity, while the shoulder at 742 nm (typically attributed to J-type aggregates [30]) completely disappeared. The B band also slightly increased in intensity at 345 nm and decreased in its shoulder at 370 nm, eventually becoming more narrow.

The inset in Fig. 6a shows the normalized changes in the absorbance of the bands during the step-wise potential change from 0.32 to −0.18 V vs Ag/AgCl. The curves resulted in an average half-wave potential of 0.00 ± 0.01 V vs. Ag/AgCl (or −0.58 V vs. Fc^+/Fc). This value is higher by 0.7 V than the formal potential for the first reversible reduction process (−1.28 V vs. Fc^+/Fc, Table 1) and lower by 0.75 than the formal potential for the first oxidation. The observed potential of the spectroscopically observed transition can be explained by an assumption that a freshly prepared solution contained some traces of the oxidized complex in an aggregated form. These aggregates stabilized the oxidized form, thus, requiring a substantial overpotential to reduce it. Close inspection of the CV data reveals some suppression of the reverse (reduction) peak for Ox_1 and additional vague reduction peaks at the reverse scan at potentials around 0.25 V vs. Ag/AgCl, *i.e.* 0.5 V lower than the formal potential of Ox_1 (Fig. 3). This may correspond to the reduction of aggregated oxidized form in agreement with the spectroelectrochemical experiment.

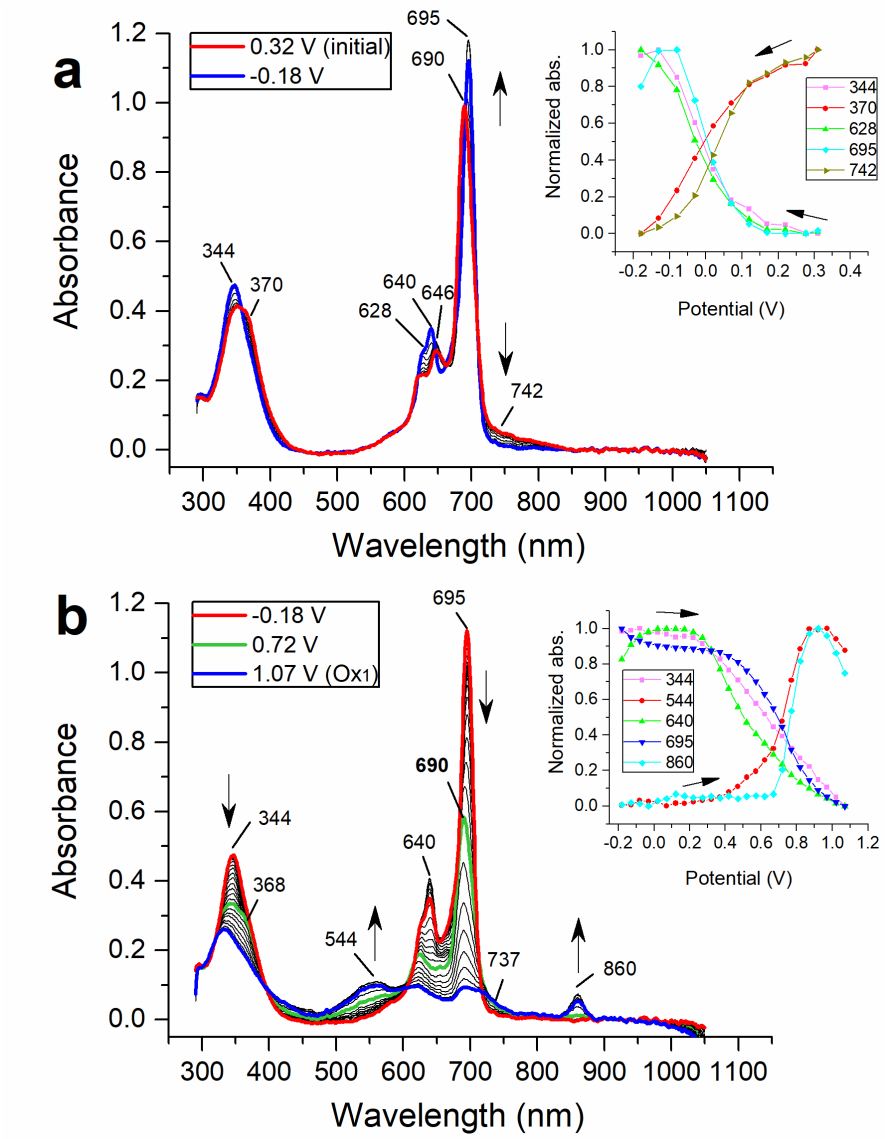

Figure 6. The effect of conditioning the solution at gradually decreased potentials from OCP (*ca.* 0.35 V) till −0.2 V that is still above the first reduction potential Red_1 (*ca.* −0.7 V) (a). In-situ UV-Vis spectral changes of ^{tBu}PcAlCl in the region of the first oxidation transition Ox_1 after preconditioning at -0.18 V (b). Other conditions were the same as in Fig. 5.

When the electrochemically preconditioned complex was oxidized stepwise until the potential of 1.10 V (Fig. 6b), the Q-band satellite at 646 nm and the band of J-aggregates at 737 nm appeared again but only at potentials 0.65—0.85 V vs. Ag/AgCl that corresponded to Ox_1 (0.76 V vs. Ag/AgCl). The Q-band also slightly shifted with the potential reaching 690 nm by 0.72 V (Fig. 6b), and a shoulder of the B-band (*ca.* 370 nm) became pronounced at the same potential. The dependence of the normalized absorbance at 344, 544, 695 and 860 nm on the potential resulted in an average half-wave potential of 0.70 ± 0.02 V vs. Ag/AgCl (0.12 V vs. Fc^+/Fc), that is lower by 0.08 V than the half-wave potential for the complex without cathodic preconditioning and lower by 0.06 V than the formal potential of Ox_1 obtained from CV measurements. This thermodynamically facilitated oxidation likely

results from additional stabilization of the oxidized state by aggregates. In general, the titration curves obtained for the preconditioned complex were less steep with changes in the B and Q bands starting from 0.3—0.4 V vs. Ag/AgCl, whereas in the non-preconditioned solution the changes started from 0.6—0.7 V.

Conclusion

Electrochemical and spectroelectrochemical methods were applied to characterize the redox transitions of ^{tBu}PcAlCl. The voltammetry revealed three reductions at −1.28, −1.65 and −2.63 V vs Fc^+/Fc and two oxidations at 0.18 and 0.90 V vs. Fc^+/Fc with good electrochemical reversibility of the first oxidation and reduction processes. Addition of 5% pyridine shifted by 0.1 V the first oxidation potential towards more positive values, indicating a possible complication of the electrochemistry in *o*-DCB by aggregation. The general overview of changes in the UV-vis spectra with applied potential generally corresponded to a simple one-electron oxidation of the Pc chromophore with a single set of isosbestic points, a typical criterion to confirm uncomplicated transition involving of two species. However, the potential resolved titration curves revealed complication of the first oxidation process associated with aggregation of the neutral and oxidized forms. The data suggest that the initial solution contains aggregates of the neutral and partially oxidized forms that complicate the oxidation of PcAlCl and facilitate partial oxidation of the neutral form. We showed that the potential-resolved spectroelectrochemical titration can be a useful tool to reveal details of redox transitions in Pcs, whereas the general picture of spectral changes with time may hinder details of the transition mechanism.

Acknowledgements

The study was supported by the ERA.Net RUS plus program and funded by RFBR (project number 18-53-76006) and Plasmon Electrolight project (No. 18-53-76006 ERA, Belgium).

References:

[1] J. Mack, M.J. Stillman, Phthalocyanines: spectroscopic and electrochemical characterization, Academic Press, San Diego, 2003.

[2] T. Basova, V. Plyashkevich, F. Petraki, H. Peisert, T. Chasse, Magnetic field-induced reactions on the surface of chloroaluminum phthalocyanine thin films, J. Chem. Phys., 134 (2011) 124703.

[3] J.A. Cissell, T.P. Vaid, A.L. Rheingold, Aluminum tetraphenylporphyrin and aluminum phthalocyanine neutral radicals, Inorg. Chem., 45 (2006) 2367-2369.

[4] I.D. Burtsev, Y.B. Platonova, A.N. Volov, L.G. Tomilova, Synthesis, characterization and photochemical properties of novel octakis(p–fluorophenoxy)substituted phthalocyanine and its gallium and indium complexes, Polyhedron, 188 (2020) 114697.

[5] A.B. Sorokin, Phthalocyanine metal complexes in catalysis, Chem. Rev., 113 (2013) 8152-8191.

[6] D. Ji, X. Lu, R. He, Syntheses of cyclic carbonates from carbon dioxide and epoxides with metal phthalocyanines as catalyst, Appl. Catal., A, 203 (2000) 329-333.

[7] J. Jiang, S. Rajendiran, S. Yoon, Double ring-expanding carbonylation using an in situ generated aluminum phthalocyanine cobalt carbonyl complex, Asian J. Org. Chem., 8 (2019) 151-154.

[8] R.R. Allison, C.H. Sibata, Oncologic photodynamic therapy photosensitizers: a clinical review, Photodiagn. Photodyn. Ther., 7 (2010) 61-75.

[9] S.U. Khan, S.A. Trashin, Y.S. Korostei, T.V. Dubinina, L.G. Tomilova, S.W. Verbruggen, K. De Wael, Photoelectrochemistry for measuring the photocatalytic activity of soluble photosensitizers, ChemPhotoChem, 4 (2020) 300-306.

[10] J.-W. Seo, S.-H. Lee, J.-Y. Lee, Enhancing quantum efficiency of parallel-like bulk heterojunction solar cells, Appl. Phys. Lett., 103 (2013).

[11] N. Li, S.R. Forrest, Tilted bulk heterojunction organic photovoltaic cells grown by oblique angle deposition, Appl. Phys. Lett., 95 (2009).

[12] Y.L. Huang, Y. Lu, T.C. Niu, H. Huang, S. Kera, N. Ueno, A.T. Wee, W. Chen, Reversible single-molecule switching in an ordered monolayer molecular dipole array, Small, 8 (2012) 1423-1428.

[13] H. Song, C. Fu, N. Li, H. Zhu, Z. Peng, W. Zhao, J. Dai, L. Xing, Z. Huang, W. Chen, Y. Wang, J. Yang, K. Wu, On the shuttling mechanism of a chlorine atom in a chloroaluminum phthalocyanine based molecular switch, Phys. Chem. Chem. Phys., 19 (2017) 22401-22405.

[14] T. Basova, V. Plyashkevich, F. Petraki, H. Peisert, T. Chasse, Magnetic field-induced reactions on the surface of chloroaluminum phthalocyanine thin films, Journal of Chemical Physics, 134 (2011) 124703.

[15] H. Yanagi, S. Douko, Y. Ueda, M. Ashida, D. Woehrle, Improvement of photoelectrochemical properties of chloroaluminum phthalocyanine thin films by controlled crystallization and molecular orientation, J. Phys. Chem., 96 (1992) 1366-1372.

[16] A.V. Zasedatelev, T.V. Dubinina, D.M. Krichevsky, V.I. Krasovskii, V.Y. Gak, V.E. Pushkarev, L.G. Tomilova, A.A. Chistyakov, Plasmon-induced light absorption of phthalocyanine layer in hybrid nanoparticles: Enhancement factor and effective spectra, J. Phys. Chem. C, 120 (2016) 1816-1823.

[17] J.A. Cissell, T.P. Vaid, A.L. Rheingold, Aluminum tetraphenylporphyrin and aluminum phthalocyanine neutral radicals, Inorganic Chemistry, 45 (2006) 2367-2369.

[18] Z. Ou, J. Shen, K.M. Kadish, Electrochemistry of aluminum phthalocyanine: solvent and anion effects on UV-visible spectra and reduction mechanisms, Inorg. Chem., 45 (2006) 9569-9579.

[19] H. Homborg, K.S. Murray, Darstellung und eigenschaften anionischer fluoro-komplexe von Mg-, Zn- und Al-phthalocyanin(2−), Zeitschrift für anorganische und allgemeine Chemie, 517 (1984) 149-160.

[20] A.B.P. Lever, P.C. Minor, Electrochemistry of main-group phthalocyanines, Inorg. Chem., 20 (1981) 4015-4017.

[21] T.M. Grant, V. McIntyre, J. Vestfrid, H. Raboui, R.T. White, Z.H. Lu, B.H. Lessard, T.P. Bender, Straightforward and Relatively Safe Process for the Fluoride Exchange of Trivalent and Tetravalent Group 13 and 14 Phthalocyanines, Acs Omega, 4 (2019) 5317-5326.

[22] Ł. Łapok, M. Obłoza, M. Nowakowska, Highly thermostable, non-oxidizable indium, gallium, and aluminium perfluorophthalocyanines with n-type character, Chem. - Eur. J., 22 (2016) 12050-12060.

[23] Z. Ou, J. Shen, K.M. Kadish, Electrochemistry of aluminum phthalocyanine: solvent and anion effects on UV-visible spectra and reduction mechanisms, Inorganic Chemistry, 45 (2006) 9569-9579.

[24] W. Freyer, F. Pragst, Absorptionsspektren von π-kationenradikalen leicht löslicher metallotetraazaporphine, Zeitschrift für Chemie, 29 (1989) 23-24.

[25] E.O. Moiseeva, Y.B. Platonova, D.V. Konev, S.A. Trashin, L.G. Tomilova, Electrochemical and spectroelectrochemical properties of tetra-tert-butylphthalocyanine indium(III), Mendeleev Commun., 29 (2019) 212-214.

[26] E.P. Platonova, E.Y. Skuridin, L.S. Degtyarev, Electrochemical oxidation and reduction of tetra-4-tert-butylphthalocyanine complexes with ions of 2nd and 3rd group-metals, Zh. Obshch. Khim., 54 (1984) 925-928.

[27] V.N. Nemykin, E.A. Lukyanets, Synthesis of substituted phthalocyanines, Arkivoc, 1 (2010) 136-208.

[28] I.D. Burtsev, T.V. Dubinina, Y.B. Platonova, A.D. Kosov, D.A. Pankratov, L.G. Tomilova, Synthesis and spectral properties of iron(III) tetra-tert-butylphthalocyanine complexes, Mendeleev Commun., 27 (2017) 466-469.

[29] S.A. Mikhalenko, S.V. Barkanova, L. Lebedev, E.A. Luk'yanets, Zh. Obshch. Khim, 41 (1971) 2735-2739.

[30] A.W. Snow, The porphyrin handbook. 109 - Phthalocyanine aggregation, Academic Press, Amsterdam, 2003.

[31] A. Ogunsipe, D. Maree, T. Nyokong, Solvent effects on the photochemical and fluorescence properties of zinc phthalocyanine derivatives, Journal of Molecular Structure, 650 (2003) 131-140.

[32] A. Atsay, A. Gül, M. Koçak, Liquid state ^{15}N NMR studies of ^{15}N isotope labeled phthalocyanines, Turk. J. Chem., 40 (2016) 163-173.

[33] J.L. Sessler, J. Jayawickramarajah, A. Gouloumis, G. Dan Pantos, T. Torres, D.M. Guldi, Guanosine and fullerene derived de-aggregation of a new phthalocyanine-linked cytidine derivative, Tetrahedron, 62 (2006) 2123-2131.

[34] H. Yoshiyama, N. Shibata, T. Sato, S. Nakamura, T. Toru, Synthesis and properties of trifluoroethoxy-coated binuclear phthalocyanine, Chem. Commun., (2008) 1977-1979.

[35] Ł. Łapok, M. Obłoza, M. Nowakowska, Highly Thermostable, Non-oxidizable Indium, Gallium, and Aluminium Perfluorophthalocyanines with n-Type Character, Chemistry - A European Journal, 22 (2016) 12050-12060.

[36] A. Lever, P. Minor, Electrochemistry of main-group phthalocyanines, Inorganic Chemistry, 20 (1981) 4015-4017.

[37] I. Noviandri, K.N. Brown, D.S. Fleming, P.T. Gulyas, P.A. Lay, A.F. Masters, L. Phillips, The decamethylferrocenium/decamethylferrocene redox couple: a superior redox standard to the ferrocenium/ferrocene redox couple for studying solvent effects on the thermodynamics of electron transfer, J. Phys. Chem. B, 103 (1999) 6713-6722.

[38] I. Noviandri, K.N. Brown, D.S. Fleming, P.T. Gulyas, P.A. Lay, A.F. Masters, L. Phillips, The Decamethylferrocenium/Decamethylferrocene Redox Couple: A Superior Redox Standard to the Ferrocenium/Ferrocene Redox Couple for Studying Solvent Effects on the Thermodynamics of Electron Transfer, Journal of Physical Chemistry B, 103 (1999) 6713-6722.

[39] A.B.P. Lever, S.R. Pickens, P.C. Minor, S. Licoccia, B.S. Ramaswamy, K. Magnell, Charge-transfer spectra of metallophthalocyanines: correlation with electrode potentials, J. Am. Chem. Soc., 103 (1981) 6800-6806.

[40] V. Manivannan, W.A. Nevin, C.C. Leznoff, A.B.P. Lever, Electrochemistry and spectroelectrochemistry of polynuclear zinc phthalocyanines: Formation of mixed valence cation radical species, J. Coord. Chem., 19 (1988) 139-158.

[41] N. Kobayashi, H. Lam, W.A. Nevin, P. Janda, C.C. Leznoff, T. Koyama, A. Monden, H. Shirai, Synthesis, spectroscopy, electrochemistry, spectroelectrochemistry, Langmuir-Blodgett film formation, and molecular orbital calculations of planar binuclear phthalocyanines, J. Am. Chem. Soc., 116 (1994) 879-890.

[42] T. Nyokong, Z. Gasyna, M.J. Stillman, Phthalocyanine π-cation-radical species: photochemical and electrochemical preparation of $[ZnPc(-1)]^{-+}$ in solution, Inorg. Chem., 26 (1987) 548-553.

[43] A.J. Bard, L.R. Faulkner, Electrochemical methods. Fundamentals and applications, 2001.

[44] E.N. Tarakanova, O.A. Levitskiy, T.V. Magdesieva, P.A. Tarakanov, V.E. Pushkarev, L.G. Tomilova, Cerium bis(tetradiazepinoporphyrazinate): synthesis and peculiarities of spectral and electrochemical behavior, New J. Chem., 39 (2015) 5797-5804.

[45] L.G. Tomilova, S.S. Talismanov, Complex compounds of cobalt (II), rhodium (III), zinc (II), and copper (II) with tetra-tert-butylphthalocyanine, Russ. J. Coord. Chem., 24 (1998) 24-31.

[46] E.R. Milaeva, G. Speier, A.B. Lever, Phthalocyanines: Properties and Applications. The redox chemistry of metallophthalocyanines in solution, VCH Publishers, Inc. , New York, 1992.

[47] T.V. Dubinina, E.O. Moiseeva, D.A. Astvatsaturov, N.E. Borisova, P.A. Tarakanov, S.A. Trashin, K. De Wael, L.G. Tomilova, Novel 2-naphthyl substituted zinc naphthalocyanine: synthesis, optical, electrochemical and spectroelectrochemical properties, New J. Chem., 44 (2020) 7849-7857.

Figures and Tables Captions

Table 1. Oxidation/reduction potentials ($E^{o\prime} \pm 0.01$ V vs. Fc^+/Fc) and the electrochemical HOMO-LUMO gaps (the difference between first oxidation and reduction potentials, ΔE).

Figure 1. Structure of tetra-*tert*-butylphthalocyanine aluminum (III), ^{tBu}PcAlCl.

Figure 2. UV-Vis absorption spectra of ^{tBu}PcAlCl (c ~ 0.01 mM) in *o*-DCB (red) and THF (blue).

Figure 3. (a) Cyclic and (b) square wave voltammograms of ^{tBu}PcAlCl (0.6—1.0 mmol/l) at a Pt-disk electrode in *o*-DCB/$TBAClO_4$; CVs scan rate: 100 mV/s. SWV amplitude 50 mV; step potential, 5 mV.

Figure 4. (a,d) Cyclic voltammograms of ^{tBu}PcAlCl in o-DCB/0.1 M $TBAClO_4$ at 0.01-2 V/s. (c,d) Trumpet plots of the peak potential, E_p, versus the logarithm of the scan rate, v. (c) Anodic peak current, i_a, and (f) cathodic peak current, i_c, plotted versus the square root of the scan rate v.

Figure 5. In-situ UV-Vis spectral changes of ^{tBu}PcAlCl (c ~ 0.15 mmol) in *o*-DCB containing 0.1 M $TBAClO_4$ in the region of the first oxidation transition Ox_1 (a) and the second oxidation transition Ox_2 (b).

Figure 6. The effect of conditioning the solution at gradually decreased potentials from OCP (*ca.* 0.35 V) till −0.2 V that is still above the first reduction potential Red_1 (*ca.* −0.7 V) (a). In-situ UV-Vis spectral changes of ^{tBu}PcAlCl in the region of the first oxidation transition Ox_1 after preconditioning at -0.18 V (b). Other conditions were the same as in Fig. 5.